

Unusual geologic evidence of coeval seismic shaking and tsunamis shows variability in earthquake size and recurrence in the area of the giant 1960 Chile earthquake



M. Cisternas^{a,*}, E. Garrett^{b,c}, R. Wesson^d, T. Dura^{e,f}, L.L. Ely^g

^a Escuela de Ciencias del Mar, Pontificia Universidad Católica de Valparaíso, Valparaíso, Chile

^b Geological Survey of Belgium, Royal Belgian Institute for Natural Sciences, Brussels, Belgium

^c Department of Geography, Durham University, UK

^d U.S. Geological Survey, Golden, CO, USA

^e Sea Level Research, Department of Marine and Coastal Sciences, Rutgers University, USA

^f Institute of Earth, Ocean and Atmospheric Sciences, Rutgers University, USA

^g Department of Geological Sciences, Central Washington University, Ellensburg, WA, USA

ARTICLE INFO

Article history:

Received 10 August 2016

Received in revised form 2 December 2016

Accepted 13 December 2016

Available online 19 January 2017

Keywords:

Paleoseismology

Tsunami geology

Earthquake recurrence

Variable rupture mode

1960 Chile earthquake

ABSTRACT

An uncommon coastal sedimentary record combines evidence for seismic shaking and coincident tsunami inundation since AD 1000 in the region of the largest earthquake recorded instrumentally: the giant 1960 southern Chile earthquake (Mw 9.5). The record reveals significant variability in the size and recurrence of megathrust earthquakes and ensuing tsunamis along this part of the Nazca–South American plate boundary. A 500-m long coastal outcrop on Isla Chiloé, midway along the 1960 rupture, provides continuous exposure of soil horizons buried locally by debris-flow diamicts and extensively by tsunami sand sheets. The diamicts flattened plants that yield geologically precise ages to correlate with well-dated evidence elsewhere. The 1960 event was preceded by three earthquakes that probably resembled it in their effects, in AD 898–1128, 1300–1398 and 1575, and by five relatively smaller intervening earthquakes. Earthquakes and tsunamis recurred exceptionally often between AD 1300 and 1575. Their average recurrence interval of 85 years only slightly exceeds the time already elapsed since 1960. This inference is of serious concern because no earthquake has been anticipated in the region so soon after the 1960 event, and current plate locking suggests that some segments of the boundary are already capable of producing large earthquakes. This long-term earthquake and tsunami history of one of the world's most seismically active subduction zones provides an example of variable rupture mode, in which earthquake size and recurrence interval vary from one earthquake to the next.

© 2016 Elsevier B.V. All rights reserved.

1. Introduction

As departures from recent historical experience, the 2004 Indian Ocean and 2011 Tohoku earthquakes and tsunamis underscore the importance of using geological evidence to help estimate the variability among earthquakes that a given subduction zone can produce (Satake, 2014). Variable rupture mode, in which a long segment of a subduction zone sometimes ruptures in a single great earthquake, but in other times ruptures in a series of relatively smaller earthquakes (Kanamori and McNally, 1982), was inferred decades ago from written records of earthquakes between AD 684 and 1946 in southwest Japan (Ando, 1975), from instrumental records of earthquakes between 1906 and 1979 in Colombia and Ecuador (Kanamori and McNally, 1982), and later from geological evidence for earthquakes at several subduction zones (see Satake and Atwater, 2007).

This paper explores variation in rupture mode in the region of the largest earthquake ever recorded instrumentally—the giant 1960 mainshock, Mw 9.5, in south-central Chile (Fig. 1). A variable behavior was previously inferred for this region by comparing historical earthquakes of 1575, 1737, 1837, and 1960 with stratigraphic evidence for land-level change and tsunamis from estuaries (Cisternas et al., 2005; Ely et al., 2014; Garrett et al., 2015; Hong et al., 2016), and with evidence for shaking in lakes of the Andean foothills (Moernaut et al., 2007; Moernaut et al., 2014). These previous findings reinforce written evidence indicating that the 1575 and 1960 earthquakes resembled one another, and that both exceeded the relatively smaller 1737 and 1837 earthquakes in fault-rupture area.

Our work focuses on an uncommon combination of stratigraphic evidence for seismic shaking and coincident tsunami inundation since AD 1000 at Cocolu on Isla Chiloé (Figs. 2–5). Geological traces of shaking and tsunamis are rarely found together; in a notable exception, sand blows from sediment liquefaction contributed to the 2011 tsunami deposit on the Sendai Plain (Goto et al., 2012). The Cocolu stratigraphy

* Corresponding author.

E-mail address: marco.cisternas@pucv.cl (M. Cisternas).

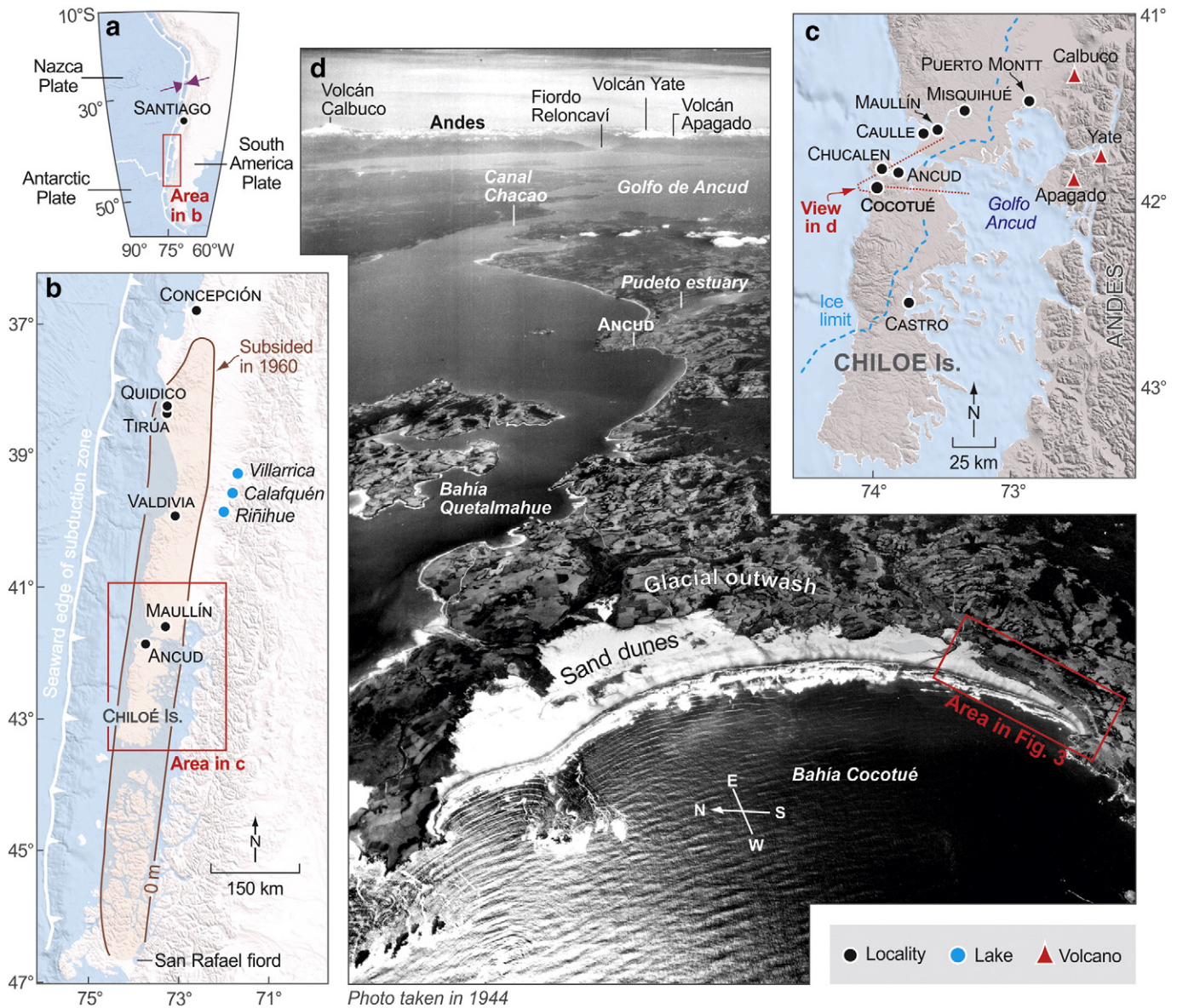


Fig. 1. Index maps and pre-1960 aerial view of the study area. a) Plate-tectonic setting of Chile. Purple paired arrows indicate plate convergence of 6.6 cm yr^{-1} (Angermann et al., 1999). b) Area of 1960 earthquake. Brown elongated ellipse outlines the area that subsided tectonically in 1960 (Plafker and Savage, 1970). Black dots mark places mentioned in the text. Blue dots mark Andean lakes studied by Moernaut et al. (2014). c) Location of Cocotué. Dashed blue curve shows western limit of the last glacial advance (Porter, 1981). d) Oblique 1944 air view of Cocotué and surroundings.

suggests the sequence of events cartooned in Fig. 2: (a) An earthquake triggers a debris flow on the former sea cliff, either for the first time or by destabilizing a scarp made by a previous earthquake. (b) The resulting debris-flow diamict covers soil at the foot of the slope, where it flattens and buries plants that had been growing there. (c) An ensuing tsunami entrains sand as it comes ashore and continues onto the toe of the debris-flow fan. The resulting sand sheet tapers across the diamict and locally entrains some of its clasts. (d) A new soil develops above both the tsunami sand and the debris-flow deposits. (e) This sequence repeats each time an earthquake sets off another debris flow followed by a tsunami.

We combine the Cocotué stratigraphic record with previously reported geological and historical evidence elsewhere in the 1960 region to reconstruct an earthquake history spanning the last 1000 years (Fig. 6). We propose that three earthquakes since AD 1000 resembled the 1960 mainshock in fault-rupture area, and that five other earthquakes likely radiated from smaller ruptures.

2. Setting

2.1. Cocotué outcrop

Our new geologic findings come from a previously undescribed outcrop along the beach on the Pacific coast at Cocotué, on Isla Chiloé (Figs. 1, 3, S1). The site is midway along the length of the 1960 mainshock rupture. The outcrop was incised by a migrating creek and ocean waves that eroded into a low terrace at the foot of a former sea cliff. The cliff, about 40 m high and composed of Pleistocene glacial outwash, was cut in the late Holocene (Heusser and Foster, 1977; Porter, 1981; Heusser, 1990). The low terrace stands about 3 m above present sea level (Fig. 4) despite about 1 m of subsidence in 1960 (Plafker and Savage, 1970). Campaign GPS measurements 13 km to the northwest show that the coast subsided 6 mm per year between 2005 and 2009 (Moreno et al., 2011).

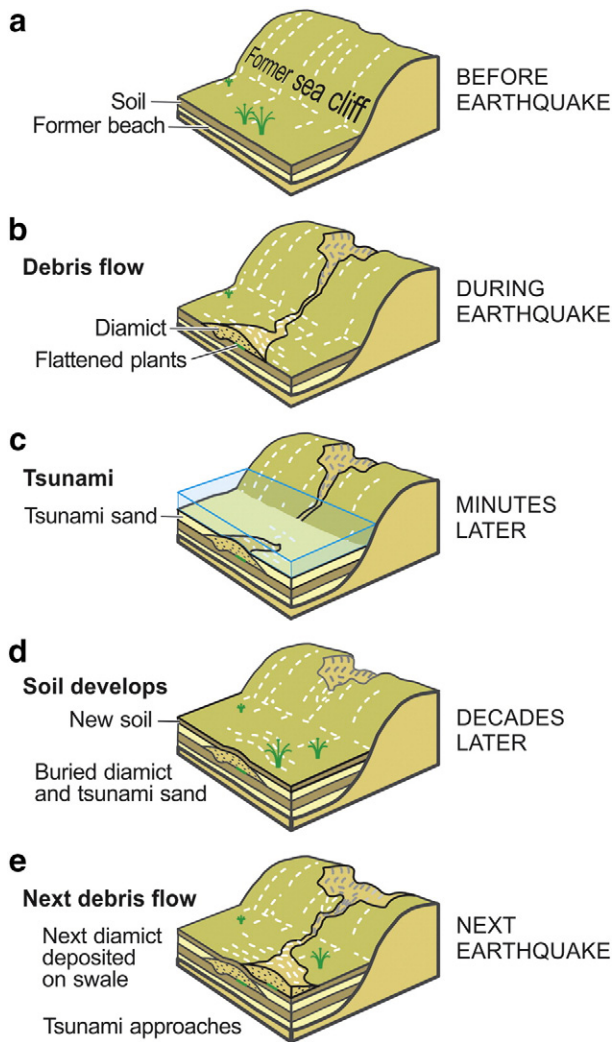


Fig. 2. Schematic view of how seismic shaking and tsunami inundation were recorded at Cocotué. a) An earthquake triggers a debris flow on a former sea cliff. b) The diamict resulting from the debris flow covers the soil at the foot of the slope, where it flattens and buries plants. c) An ensuing tsunami entrains sand as it comes ashore, and subsequently deposits the sand on the toe of the debris-flow fan. d) A new soil develops on the tsunami deposit and the diamict. e) The next cycle begins when another earthquake triggers another debris flow.

Although the terrace is formed on beach deposits, its rear portion is covered by a seasonal freshwater pond, and the rest by land plants, including shrubs and herbs (Figs. 3, S1). Below we show that freshwater conditions have probably prevailed for most or all of the roughly 1100 years since a soil began to form on the beach deposits.

The 22 May 1960 earthquake triggered debris flows on the face of the former sea cliff and elsewhere on Chiloé as shown by airphotos taken in January 1961 (Fig. 3b). The Cocotué outcrop cuts across the toes of the 1960 and earlier debris-flow fans, and also exposes intercalated sand sheets (Fig. 3c).

2.2. Earthquake and tsunami written history in the 1960 area

Written records report at least three predecessors to the 1960 earthquake (Lomnitz, 1970; Cisternas et al., 2005). The earliest of these, in 1575, most closely resembles the 1960 mainshock based on the spatial extent and severity of its effects. The shaking in 1575 damaged Spanish settlements from Concepción to Castro (Fig. 1), and it triggered landslides that blocked the outlet of Riñihue Lake in the Andean foothills. Five months later an outburst flood killed thousands of natives and inundated Valdivia, 80 km downstream (Lomnitz, 1970). The 1575

earthquake was also associated with a tsunami that took >1000 lives north of Valdivia and wrecked galleons in that city's port.

The poorly known next predecessor, in 1737, reportedly damaged Valdivia and towns of Isla Chiloé but no associated tsunami has been reported (Cisternas et al., 2005). By contrast, the central Chile earthquakes of 1730 and 1751 farther to the north were both associated with tsunamis that were noted not just in Chile (Lomnitz, 2004; Udías et al., 2012) but also in Japan (Watanabe, 1998).

The most recent predecessor to the 1960 earthquake, in 1837, destroyed buildings midway along the 1960 rupture area. It was accompanied by changes in coastal land level farther south that lowered some islands (Vidal Gormaz, 1877) while raising others (Darwin, 1851). The ensuing tsunami appears to have been relatively small where documented at Chiloé but crested 6 m high in Hilo, Hawaii (Coan, 1882) and caused flooding and damage near Sendai, Japan (Watanabe, 1998). On the basis of the tsunami's height in Hilo, the 1837 earthquake was assigned a tsunami magnitude of 9 1/4 (Abe, 1979).

2.3. The 1960 earthquake

The mainshock of 22 May 1960 resulted from a rupture at the boundary between the subducting Nazca plate and the overriding South America plate following an extraordinary series of foreshocks (Cifuentes, 1989; Fig. 1a). The mainshock produced extensive damage and abundant slope failures in most of south-central Chile (Weischet, 1963). Warping of the overriding plate lowered one-quarter of Chile's outer coast by a meter or two (Plafker and Savage, 1970; Fig. 1b). Concurrent displacement of the seafloor generated a tsunami with peak heights of 15 m in Chile (Sievers, 1963), 10 m Hawaii (Eaton et al., 1961) and 6 m in Japan (Watanabe, 1998).

3. Previous work

Paleoseismological studies have extended the history of earthquakes and tsunamis in south-central Chile thousands of years into the past. Some of these studies have relied on evidence for coastal land-level changes and tsunamis, while others have used evidence for shaking. So far none has combined both types of evidence for the same event.

3.1. Land-level changes and tsunamis

Midway along the 1960 earthquake rupture area, reconnaissance studies in the late 1980s uncovered coastal evidence for its predecessors in the Maullín estuary, located on the mainland 50 km north of Cocotué (Fig. 1). Buried soils provided evidence for recurrent subsidence despite net late Holocene emergence of tidal-marshes (Atwater et al., 1992). Further study yielded a 2000-yr history of repeated coseismic subsidence and tsunamis (Cisternas et al., 2005). The average interval between 1960-type events was two to three times longer than the 128-year average interval separating the 1575, 1737, 1837, and 1960 events. The youngest four events in the Maullín sequence (D, C, B, and A), each marked by subsidence and tsunami, occurred within the past 1000 years. Radiocarbon analyses dated event D to AD 1020–1180 and event C to AD 1280–1390. Maullín event B likely corresponds to 1575 and event A is unquestionably 1960. Traces of subsidence and tsunamis in 1737 and 1837 were sought but not found at the estuary. Indeed, there is a widespread absence of buried soils intermediate between those conspicuously preserved from 1575 and 1960. In addition, tree-ring (see below) and written evidence argued against 19th-century subsidence.

Landforms and pits on a beach-ridge plain at Caille, 7 km southwest of Maullín, provided stratigraphic evidence for three tsunamis, including the one in 1960 (Atwater et al., 2013). The site, two kilometers inland, includes a breach in a Holocene beach ridge, a pond that extends landward from the breach, and a fan that partly rims the pond. At least two tsunamis prior to 1960 cut the breach. The 1960 tsunami

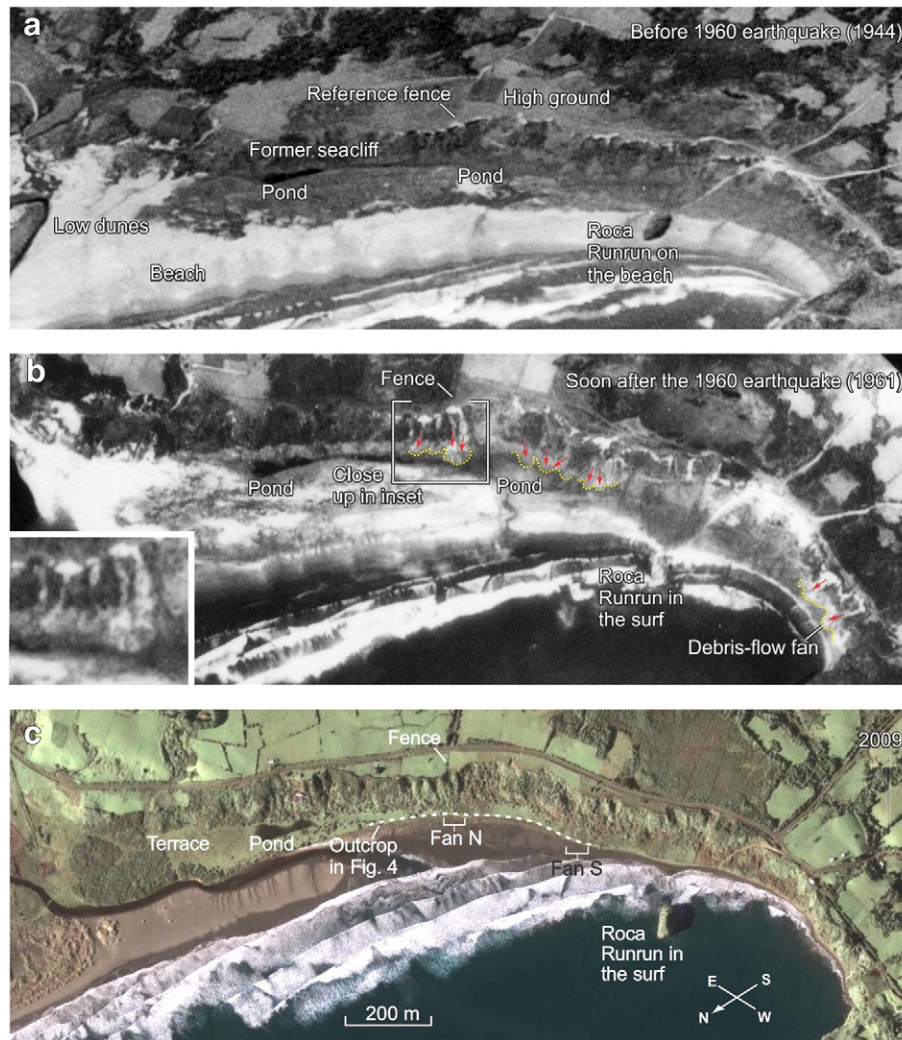


Fig. 3. Setting of the Cocotué outcrop shown by aerial views before and after the 1960 earthquake and tsunami (see also Fig. S2). a) Oblique 1944 airphoto shows the slope of the former sea cliff and the elongated freshwater pond at its foot. All three views show the same fence line. In 1944, the sea stack known as Roca Runrun was surrounded by beach sand. b) Vertical airphoto taken eight months after the 1960 earthquake shows a series of fresh debris-flow channels and associated fans. Some of them are enlarged in the inset. Yellow dotted line and small red arrows indicate the distal limits of the debris-fan fronts. Coseismic subsidence (~1.5 m) and consequent shoreline retreat have left Roca Runrun in the surf. c) An image from 2009 shows that most of the southern pond area had been eroded and the shoreline had retreated to intersect the debris-flow fans. Dashed white line shows the outcrop mapped in Fig. 4a (image © Digital Globe).

reamed out the breach and aggraded the fan with a sedimentary breccia of sand and soil clasts. Two older sand deposits were found below the 1960 soil, each resting on buried soils. Dating gave an age of AD 1270–1400 for the lower sand bed, similar to the age range of Maullín event C (AD 1280–1390). The intermediate sand sheet was stratigraphically ascribed to the 1575 tsunami.

Coastal evidence for recurring earthquakes was also identified at Chucalén, an estuarine site 10 km north of Cocotué on the sheltered coast of northern Chiloé (Garrett et al., 2015; Fig. 1c). Four buried soils, at least three of them capped with a sand sheet, provide evidence of earthquakes and tsunamis in 1960 and 1575 and at two earlier times overlapping the ages of Maullín's events C and D. Changes in diatom assemblages show that subsidence coincided with at least three of the earthquakes. As in Maullín, no geologic evidence of the historical earthquakes in 1737 and 1837 was found in Chucalén.

Evidence of land-level change and tsunamis also has been found in the northern half of the 1960 rupture area. Cores in marshes of the Valdivia estuary (Fig. 1b), 230 km north of Cocotué, encountered fragmentary evidence of subsidence and tsunamis before 1960 (Nelson et al., 2009). This evidence includes two successive buried soils that are each overlain by sand and were dated to 2700–1700 and 1700–1300 cal yr BP.

Estuarine stratigraphy at Tirúa (Fig. 1b), 400 km north of Cocotué, shows four instances of land-level change and accompanying tsunamis over the past 450 years within the overlapping ruptures areas of the 1960 and 2010 earthquakes (Ely et al., 2014). Negligible subsidence reported in 1960 at Tirúa (Plafker and Savage, 1970) contrasts with the uplift of 0.5–1 m of this area during the 2010 earthquake. Likewise Tirúa appears to have subsided during the southern Chile earthquake of 1575 and to have been uplifted during the 1751 earthquake to the north. Based on multiple radiocarbon ages and stratigraphic position, Ely et al. (2014) ascribe one of the sand sheets at Tirúa to the 1575 tsunami. Yet, OSL dating suggests older ages (AD 1390 ± 80) for this and other sand sheets in the sequence (Nentwig et al., 2015).

Evidence of five tsunamis was found in an abandoned meander and banks of Quidico River, 10 km north of Tirúa (Hong et al., 2016). All events but the oldest were correlated with historical tsunamis in 2010, 1960, 1835 and 1751. Although Quidico lies near the northern boundary of the 1960 region, its sequence appears to record tsunamis sourced in the 2010 earthquake region. A prehistoric tsunami dated to AD 1445–1490 is marked by a thick and widespread sand sheet. Its source remains unknown.

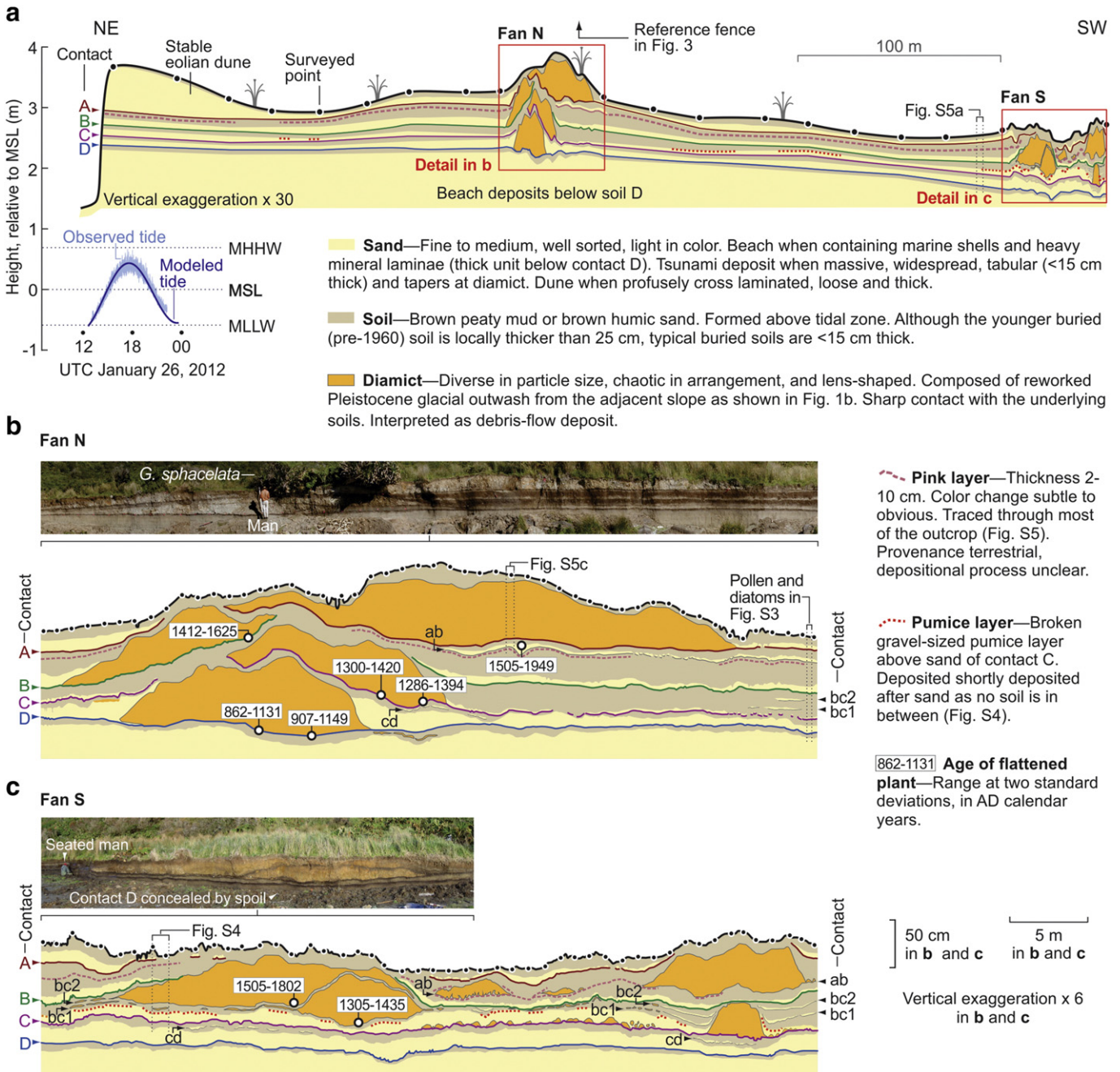


Fig. 4. Stratigraphy at Cocotué. a) Stratigraphic cross section of the entire surveyed outcrop. b and c) Details of the toes of fans N and S. Most of the ages were measured on the remains of plants in growth-position that had been flattened by debris flows.

Further clues about land-level changes come from arboreal evidence. Drowned forests of dead or dying trees at San Rafael fiord (Fig. 1b), at the southern end of the 1960 rupture, provided evidence for subsidence in 1837. Counting the annual growth rings of one drowned tree, still rooted to the floor of the fiord, Reed et al. (1988) noted it became stunted and tilted in the 1830s. Comparing the level of the lowest healthy living trees with the level of the lowest well preserved dead stumps, they inferred a subsidence between 2.0 and 2.5 m.

In contrast, old-growth trees in northern Chiloé and near Maullín, killed or damaged by tidal submergence after subsiding in 1960, show no evidence of subsidence in 1837. Measuring tree diameters and annual rings, Bartsch-Winkler and Schmoll (1993) suggested that a forest drowned in 1960 at the Pudeto estuary of Chiloé (Fig. 1d) had failed to subside in 1837. On the mainland at Misquihué (Fig. 1c) a similar

story was inferred counting rings of 15 trees killed in 1960. Ten of them were found to have lived through 1837 and two through 1737 as well (Cisternas et al., 2005). Furthermore, on an 1874 nautical chart, Chilean Navy surveyors schematically depicted the Misquihué trees as large and healthy.

3.2. Geologic evidence for shaking

Shaking-triggered turbidites at Puyehue Lake (Fig. 1b), in the foothills of the Andes and about 150 km northeast from Cocotué, provide evidence for nine earthquakes comparable to the 1960 event during the last 10,000 years (Moernaut et al., 2007). Although shaking had recurred at irregular intervals, spanning 1000 years on average, the two

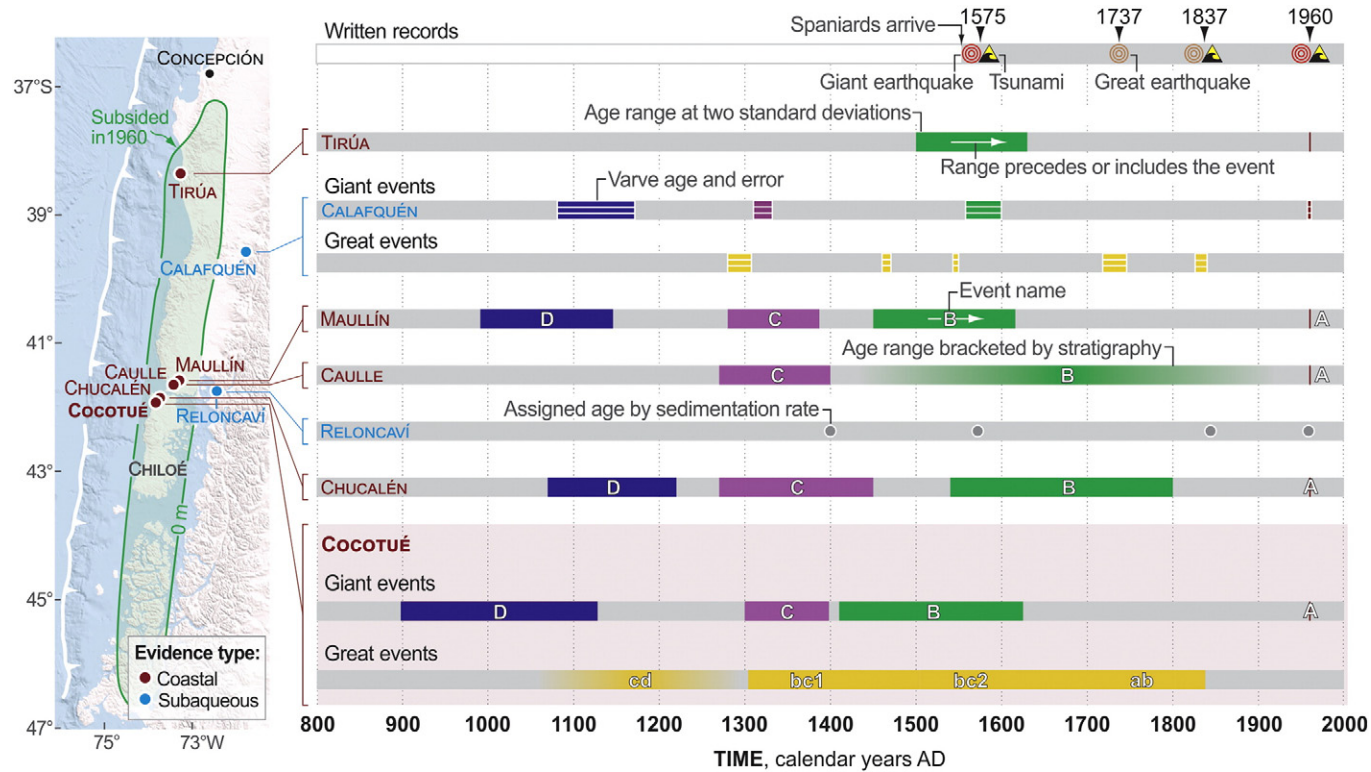


Fig. 5. Chronologic comparison, from north (top) to south (bottom), of evidence for earthquakes and tsunamis along the length of the 1960 region. No data coverage south of Chiloé. Written records from Lomnitz (1970), Cisternas et al. (2005) and Fig. 6 of this report. Filled rectangles for Tirúa, Maullín, Caulle, Chucalén and Cocotué show age ranges of plant fossils at two standard deviations (Ely et al., 2014; Cisternas et al., 2005; Atwater et al., 2013; Garrett et al., 2015). Cocotué ages from coastal sand sheets and diamicts, interpreted as recording giant and merely great events (this report). Colors of the rectangles match the events that have been previously correlated, by stratigraphy and dating, to the events of Maullín—Blue: event D; purple: C; green: B (1575); red: A (1960). Gray dots for Reloncaví indicate dates of earthquakes inferred from marine turbidites and average sedimentation rates (St-Onge et al., 2012). Barred rectangles show dates and uncertainty derived from varve counts for turbidites in Calafquén Lake (Moernaut et al., 2014). Basin-wide and local turbidites interpreted as produced by large and smaller events respectively.

youngest turbidites were linked to the historical earthquakes of 1575 and 1960.

By contrast, turbidites off the Chilean coast between 38°S and 40°S suggest a more frequent earthquake recurrence, every 100–200 years, over the last glacial period (Blumberg et al., 2008). Climate, sea-level change and proximity to the seismic source would explain such a short recurrence interval by promoting the triggering of offshore turbidites, which likely recorded earthquakes of different sizes. Similar influences were inferred by Bernhardt et al. (2015) when studying offshore turbidites in central Chile, between 29°S and 38°S. Although two of the Bernhardt et al. (2015) cores are located in the northern end of the 1960 region, the scarcity of planktonic foraminifera in the hemipelagic intervals did not allow a well resolved chronology to compare with other available paleoseismic records.

The 1575, 1837 and 1960 earthquakes have been invoked to explain a series of three turbidites in another marine record at Reloncaví Fjord (Fig. 1d), 120 km east of Cocotué (St-Onge et al., 2012). Turbidites were linked to those historical dates through average sedimentation rates. A fourth and deeper turbidite was attributed to an earthquake around AD 1400.

Turbidites found in lakes Villarica, Calafquén and Riñihue (Fig. 1b), along the northern half of the 1960 region, suggest variation in rupture mode over the last 900 years (Moernaut et al., 2014). The turbidites were stratigraphically correlated within each of the three lakes. Successive turbidites differed in spatial extent and thickness, characteristics interpreted as products of local earthquake intensity. Although lacking evidence from the southern half of the 1960 rupture area, the four turbidites were ascribed to earthquakes that ruptured its entire along-strike length in AD 1083–1171, 1310–1332, 1575 and 1960. This turbidite sequence improves upon the less precisely constrained ages for the prehistoric events D and C in the Maullín earthquake history (Cisternas et al., 2005). Additionally, intervening smaller turbidites in one basin of Calafquén Lake were interpreted as three smaller events, in AD 1280–1308, 1460–1470 and 1544–1548 (Moernaut et al., 2014). Of the three, only the AD 1460–1470 has a counterpart in another lake, at Riñihue. Two younger and smaller turbidites were linked to the historical earthquakes of 1737 and 1837. The extent and thickness of these turbidites, compared with other paleoseismic and historical records, suggest a northern rupture in 1737 and a southern rupture in 1837.

4. Methods

4.1. Stratigraphy

We found the Cocotué exposure during the austral summer of 2006 and studied it further during the summers of 2007, 2008 and 2012. Using picks and shovels we cleaned an outcrop 500 m long. Stratigraphic logs were made every 10 m for most of the exposure and every 1 m at debris-flow fans. Grain size and texture were estimated in the field by hand lens.

Airphotos taken before and soon after the 1960 earthquake aided in developing the interpretations cartooned in Fig. 2. Pre-earthquake oblique airphotos were taken by the United States military in 1944 and post-earthquake vertical airphotos were taken by the Chilean airforce in January 1961 (Figs. 1d, 3).

4.2. Topography and sea level

Height differences among features in the outcrop were measured during each field season with a tripod-mounted level. The points surveyed in this manner were referred to a common benchmark by means of third-order leveling with a closure error of 1 cm.

In January 2012 we linked the benchmark level to mean sea level. We estimated mean sea level at Cocotué by measuring the water level continuously for 10 h with a portable acoustic tide gauge that we

referenced to the benchmark. The resulting tide record, obtained at a time of fair weather, was fitted to tidal predictions from the TPXO 8-atlas tidal model, which is based on harmonic constituents extracted from 14 years of TOPEX/Poseidon satellite altimetry (Egbert et al., 1994; Egbert and Erofeeva, 2002; Melnick et al., 2012). The inferred total error in the estimate of mean sea level at Cocotué was <0.1 m.

4.3. Dating by radiocarbon and introduced pollen

Accelerator mass spectrometry (AMS) radiocarbon analysis provided ages for the plants flattened and buried by the debris flows. Well-preserved plant remains, mainly of pineapple-like bromeliads (*Greigia sphacelata*) and rushes (*Juncus* sp.) were found bent seaward, in about the same direction as the debris-flow runout in 1960. We collected the samples by detaching the overlying diamict from the underlying soil (Fig. S2). Living *G. sphacelata* plants, which still grow on the debris-flow fans, have hard and thorny leaves—a characteristic that likely promoted their preservation. Other dated organic material included a delicate twig, a small root of a bush likely overrun by the debris flow, and a piece of wood within the second-youngest sand sheet. All the radiocarbon ages were calibrated to years AD at two standard deviations. For calibration we used the Southern Hemisphere data set of Hogg et al. (2013) and the software Calib Rev 7.0 (<http://www.calib.qub.ac.uk/calib/>).

We used pine pollen to assess the age of sediment deposited in the late 19th and early 20th centuries (Cisternas et al., 2001). Chile had no pine trees until *Pinus radiata* was first planted in the Concepción area in 1885 (Aztorquiza, 1929; Donoso and Lara, 1996). It expanded early in the 20th century under a policy of the national government (Contesse, 1987). We therefore assume that pine pollen at Chiloé became abundant no earlier than 1900. We looked for pine pollen in the upper soils of the Cocotué stratigraphy by analyzing 1-g samples taken 1 cm apart. Samples were processed with standard palynological techniques (Faegri and Iversen, 1975; Dupré, 1992). Pollen concentrations, in grains per gram, were measured with the methods of Anderson (1974) and Kempt et al. (1974).

4.4. Diatom paleoecology

Fossil diatoms in coastal sedimentary sequences help to reconstruct past relative sea levels and determine sediment provenance (Hemphill-Haley, 1996; Dawson, 2007; Dura et al., 2016). Along the Cocotué's outcrop we selected an undisturbed stratigraphic column to be sampled for diatoms (location in Fig. 4b). Diatoms were extracted, using standard preparation methods (Palmer and Abbott, 1986), from 0.5 cm thick samples from the soils and sand sheets that bracket them. We inspected slides at a magnification of $\times 1000$, identifying at least 250 diatom valves per sample. Identifications followed Rivera and Valdebenito (1979), Hartley et al. (1996) and reference collections held by Durham University. We inferred the paleoecology of the assemblages by grouping species into five categories based on their salinity preference, in the manner of Lowe (1974), Hemphill-Haley (1993), and van Dam et al. (1994).

5. The Cocotué stratigraphy

The overall stratigraphy along the 0.5-km-long Cocotué outcrop includes four nearly continuous, mostly tabular units of fine clean sand, each averaging about 10 cm in thickness. These sand sheets alternate with dark organic soil layers, ≥ 10 cm thick, which give the exposure a horizontally banded appearance (Fig. 4). This sequence rests on a basal unit of beach sand. Since surveyed, the exposure has been eroded by waves and partially collapsed.

Sharp contacts mark the boundaries between each sand sheet and underlying soil. These four distinct and continuous sand-soil contacts, from youngest (top) to oldest (bottom), are termed here contacts A, B,

C, and D (Fig. 4). One of the four, contact C, is distinctive lithologically because the sand above it contains pebbles of pumice (Figs. S4, S5a). The youngest of the four, contact A, is distinctive paleontologically as the only contact that overlies pine pollen (Fig. S3b).

Diamicts, composed of unsorted mixtures of clay, silt, sand, and gravel, locally interrupt sand sheets above contacts A, B, C, and D. The largest clasts within the diamict are cobbles and boulders as much as 40 cm in diameter. These are well rounded and a few of them are so weathered that they can be cut with a knife. All these unsorted mixtures are also exposed in a landslide scarp high near the top of the former sea cliff, pointing to the cliff as the source of the diamicts. The diamicts themselves form lenticular beds that coincide with the toes of two conspicuous debris-flow fans (Fans N and S; Fig. S1). Although the diamicts locally interrupt the continuity of the sand-soil contacts, becoming diamict-soil contacts, the lack of erosion on the tops of the soils, evidenced by the presence of growth-position flattened plants (Fig. S2), persuaded us to keep the contact name through the diamict-soil contacts, even though they likely mark a different process.

Four less distinct and discontinuous additional contacts, each capped by a sand sheet and three of them also by diamicts, are present locally within the soils beneath contacts A, B, and C. Most of the less conspicuous contacts are associated with fan S but some are also found at fan N. The stratigraphically oldest of the additional contacts, termed cd, is between contact C and D. Two others, contacts bc1 and bc2, are between contact B and C. Contact ab, with a distinctively pink soil, underlies both contact A and the earliest (highest) occurrence of pine pollen (Figs. S3b, S5).

5.1. Basal beach deposits

Beach deposits thicker than 2 m underlie the eight contacts described below (Fig. 4). We ascribed this basal unit to beach because it contains scattered marine shells and heavy mineral laminae similar to those in the modern foreshore beach. On this old beach an organic dark soil developed. As the soil contains mostly freshwater, salt-intolerant diatoms and was vegetated with plants before burial (Figs. S2, S3), it probably resulted from a significant land-level change that raised the beach out of the tidal zone. The soil likely developed shortly before 1000 years ago, when its plants were buried (see age of contact D below). Freshwater species dominated diatom assemblages in the overlying sediments (Fig. S3c), implying that the terrace has never returned to the tidal reaches since the formation of the soil on the beach. Despite this broad trend, during the last 1000 years the freshwater, salt-intolerant diatoms have diminished upwards in favor of diatoms that tolerate or are stimulated at low salinity. This subtle trend would suggest either a relative sea-level rise, a net landward advance of the shore that exposed the terrace to salt spray, or both.

5.2. Contact D

Contact D marks the boundary between the soil developed on the old beach and both sand and diamict deposits (Fig. 4b). The contact is clearly delineated by a ~10-cm thick tabular sand sheet, which rests on the soil along the entire 500-m outcrop and overlaps both pinched-out edges of the diamict lens. Freshwater diatoms predominate in this sand sheet (Fig. S3c). The diamict lens, located at fan N, is the second largest in exposed area at Cocotué. No coeval diamict is evident at fan S.

Plants flattened and buried by the diamict at fan N date contact D to AD 907–1149 (*Juncus* sp.) and AD 862–1131 (*G. sphacelata*). Their pooled mean age, 1083 ± 31 14 cal yr BP, corresponds to AD 898–1128 at 2σ (Fig. 5; Tables 1, S1).

5.3. Contact cd

Contact cd is defined only by a sand-soil discontinuous boundary. No diamict lens was observed interrupting the sand sheet or occurring at

the same stratigraphic level. The thin (~3 cm) tabular and discontinuous sheet of clean sand is found 3–5 cm below contact C. Its clearest exposure is at fan S, where it extends continuously for ~4 m below the diamict that marks contact C (Fig. 4c). Contact cd also occurs discontinuously at two other locations: ~25 m northward from the first place in fan S, and hundreds of meters northward, in fan N, below the diamict of contact C (Fig. 4b).

We were not able to find adequate material to date contact cd; however, by its position, between D and C, contact cd postdates AD 898–1128 and predates AD 1300–1398 (see age of contact C below).

5.4. Contact C

Contact C is clearly marked by both sand-soil and diamict-soil boundaries. While the sand sheet is thinner (~4 cm) and broken in fan N, as it is probably trampled (Figs. 4b, S3), it is thicker (~10 cm) and continuous in fan S (Fig. 4c). The sand overlaps only the lower pinched edge of the diamict in fan N but both edges in the diamict of fan S. Of all the sand sheets at the outcrop, the sand over contact C contains the largest proportion of marine diatoms (30% of the total assemblage; Fig. S3c). Remarkably, diamict lenses over contact C occur at both of the debris-flow fans. The diamict at fan N is laterally longer than the one in fan S (Fig. 4b, c).

A distinctive but discontinuous ~5-cm-thick layer of rounded, gravel-sized pumice (1–5 cm in diameter) conformably caps the sand sheet over contact C at different places but mainly at fan S (Fig. 4a, c, S4). No soil nor erosion is evident between the sand and the pumice. Additionally, no other conspicuous pumice layer is evident in the 1000-year-long stratigraphic record. These absences suggest a closeness in time between the pumice deposition and the process that produced contact C. A short discussion about the pumice sources and a possible volcanic eruption associated to event C is in the Supporting material (Text S1).

The diamict over contact C, at fan N, flattened a twig from AD 1300–1420 and a *G. sphacelata* leaf from AD 1286–1394. The pooled mean age constrains contact C to AD 1300–1398 (Tables 1 and S1).

5.5. Contacts bc1 and bc2

Two closely spaced contacts, bc1 and bc2, are overlain by both sand and diamict deposits between contacts C and B. They are delineated by two thin (~3 cm) sand sheets that pinch out on the flanks of the soil-covered diamict that overlies contact C in fan S (Fig. 4c). The sandy pair also occurs in the middle of fan S and at the southern end of fan N. A pair of overlapped diamict lenses likely also mark contacts bc1 and bc2 between contact C and B. They show an architecture similar to that of fan N: the younger diamict occupies an area beside the higher ground created by the preceding diamict (Figs. 4c and S1d). We could not trace laterally the sand-soil contacts with the diamict-soil contacts; however, their similar stratigraphic level and spatial closeness strongly suggest their correlation.

By their position between contacts C and B, contacts bc1 and bc2 postdate AD 1300–1398 and predate AD 1411–1625 (see age of contact B below). However, radiocarbon dates obtained for bc1 and bc2 overlap those of the bracketing contacts (Table S1). The earlier diamict in the couplet, resting on contact bc1, flattened and buried a *Juncus* stem from AD 1304–1435, an age mostly indistinguishable from that of the preceding contact C (AD 1300–1398). Likewise, the later diamict, resting on contact bc2, flattened a *Juncus* stem from AD 1505–1802, a range that overlaps the age of the overlying contact B (AD 1412–1625).

5.6. Contact B

Contact B is defined by both sand-soil and diamict-soil boundaries. This contact is clearly marked by a ~8-cm thick tabular sand sheet, which rests on the soil along the entire outcrop. The sand sheet overlies

Table 1

Stratigraphic and chronological correlation between the Cocotué events (this report) and coastal (Cisternas et al., 2005; Atwater et al., 2013; Garrett et al., 2015) and subaqueous lacustrine evidence (Moernaut et al., 2014) elsewhere. Bold and regular lettering denote events interpreted as giant and relatively smaller earthquakes respectively. Asterisks indicate dates inferred from stratigraphy, written records, or airphotos. While ages from Cocotué Maullín, Caulle, and Chucalén were obtained through radiocarbon analyses, the Villarica, Calafquén, and Riñihue lakes were derived counting varves.

COCOTUE EVENT	HISTORICAL EVENT	COASTAL EVIDENCE (Years AD at 2 σ)			LACUSTRINE EVIDENCE (Years AD)			
		Cocotué	Maullín	Caulle	Chucalén	Calafquén	Riñihue	Villarica
D		898–1128	1020–1180		1070–1220	1083–1170		
cd		898–1398	1020–1387			1280–1308		
C		1300–1398	1280–1387	1270–1400	1270–1450	1310–1332	1307–1327	
bc1		1305–1435				1460–1470	1464–1471	
bc2		1505–1802				1544–1548		
B	1575	1412–1625	1450–1616	1575*	1540–1800	1558–1600	1562–1596	1558–1608
	1737					1718–1746		1723–1755
ab	1837	1505–1949				1831–1847	1826–1840	1820–1840
A	1960*	1960*	1960*	1960*	1955–1971	1958–1962	1959–1963	1957–1963

Bold and regular lettering show giant and great events respectively; * shows dates inferred from stratigraphy, written records or airphotos.

only a distal edge of the diamict lens at fan N. Like contact D, contact B is marked by only one diamict lens.

The age of contact B is limited by a woody root that was 2 cm below the surface of the soil buried by the diamict in fan N. If the root was part of a plant killed by the debris flow, the contact dates to AD 1412–1625 (Tables 1 and S1).

5.7. Contact ab

The penultimate contact at Cocotué is overlain by a relatively thick (2–6 cm) and continuous sand sheet that lies 4–8 cm below contact A at fan N (Figs. 4b, S3, S5c), and by diamict lenses in fan S. Both the diamicts and the sand overlie a conspicuous change in color in the soil (pink when wet, paler when dry; Fig. S5). On this basis, the sand at fan N was correlated with two small and one medium-size diamicts in fan S (Fig. 4c). The diamicts and sand sheet are stratigraphically closer to contact A than to contact B, which suggests a temporal proximity between those deposits and the process that produced contact A.

A piece of wood included in the sand sheet gave a maximum calendar age of AD 1505–1949, with most of the probability density between AD 1700 and 1800 (Tables 1 and S1). A further minimum age for contact ab is provided by *P. radiata* pollen (Fig. S3b). Because the sand sheet is ~4 cm below the soil that contains the deepest pine pollen, contact ab should predate AD 1900 by several decades, when widespread planting of *P. radiata* began in southern Chile.

5.8. Contact A

The youngest contact at Cocotué is clearly marked by both sand-soil and diamict-soil boundaries. It underlies a widespread and thick (~7–12 cm) sand sheet and the largest diamict lens (Fig. 4). The sand sheet is continuous through the entire outcrop and at its northeastern end is mixed with or overlapped by eolian sand, reaching almost 1 m thick. The sand sheet overlaps the southern edge of the diamict. Remarkably, this diamict extends laterally >30 m and, while lapping onto older diamicts, projects mainly to the south of them. The age of this contact is discussed below, in Section 6.2.

6. Interpretations and correlations

6.1. Stratigraphic interpretations

We interpret each of the Cocotué sand sheets as a tsunami deposit. We invoke tsunamis, instead of tidal flat, eolian or storm washover deposits, for reasons similar to those used at Maullín (Cisternas et al., 2005): similar sand grain size and texture to those of the sand

composing the modern beach, widespread tabular shape, abrupt and continuous lower contacts, and absence of bioturbation in the underlying soils. We also discount the alternative hypothesis of tidal-flat deposition because the terrace stood above high-tide level even after subsiding in 1960.

Diatoms associated with the sand sheets neither confirm nor refute a tsunami source (Fig. S3c). Freshwater assemblages predominate in most of the sand sheets. The predominance of freshwater species need not imply a terrestrial sediment source, however, because the former cliff lacks clean sand similar to that of the sand sheets. We hypothesize that sand derived from the beach may have contained few diatoms to begin with, while post-depositional freshwater ponding and infiltration may have introduced freshwater diatom taxa into the sand sheets.

We interpret each of the diamict lenses as an earthquake-triggered debris-flow deposit. This interpretation is supported by their mix of clast types and their coincidence with fans at the bases of debris-flow channels. Airphotos taken eight months after the 1960 earthquake show fan N covered by a fresh, large debris flow (Fig. 3b). Furthermore, the 1960, 1837 and 1575 earthquakes are known to have produced abundant slope failures in south-central Chile (Weischet, 1963; Davis and Karzulovic, 1963; Cisternas et al., 2005).

Where a diamict lens and a sand sheet buried the same soil, and where the sand extends onto unweathered debris-flow deposits, we infer that a tsunami was triggered during the same earthquake that set off the debris flow (Fig. 2).

When a laterally large diamict lens is associated with a continuous and relatively thick sand sheet, comparable with those assigned to the 1960 earthquake and tsunami (see below), we simplistically infer that they were more likely created by a 1960-type earthquake and tsunami. When the diamict lens is smaller and the sand sheet is discontinuous and thin, we infer that they more likely resulted from a relatively smaller or perhaps more distant event. In making a final interpretation of the relative sizes of the events at Cocotué, we also considered the latitudinal extent of correlative deposits at other sites.

Given these interpretations, and the corresponding radiocarbon ages, the series of eight contacts gives evidence of four possible 1960-type earthquakes and tsunamis (from old to young, events D, C, B, and A), and of four intervening relatively lesser events (cd, bc1, bc2, and ab) in the span of about 1000 years.

6.2. Chronological correlation with well-dated evidence elsewhere

In most cases the ages of the plants killed by debris flows predate the inferred earthquake by no more than a few years. This geological precision facilitates correlation with well-dated coastal and subaqueous evidence elsewhere and with historical accounts (Tables 1 and S1; Fig. 5).

The oldest 1960-type earthquake and tsunami recorded in Cocotué (event D), marked by the lowest debris-flow deposit and associated sand sheet, occurred in AD 898–1128. Notably this age coincides with evidence for a 1960-type earthquake and tsunami at Maullín (Cisternas et al., 2005) and Chucalén (Garrett et al., 2015), and for a comparable earthquake in Calafquén Lake (Moernaut et al., 2014). The Cocotué age range overlaps the age of two rushes killed by tidal submergence at Maullín, the modelled age of submergence at Chucalén and the age of the oldest large turbidite in Calafquén Lake (Fig. 5; Tables 1 and S1).

Sometime after event D, a relatively smaller tsunami was recorded in Cocotué (cd). Although we could not date it, by its stratigraphic position, between D and C, it postdates AD 898–1128 and predates AD 1300–1398. Interestingly, a local turbidite in Calafquén marks a smaller earthquake that coincides, by stratigraphic position and age range, with cd (Tables 1 and S1). Event cd likely also correlates with a smaller tsunami recorded in Maullín. There, at the seaward end of two perpendicular transects, a thin 1-cm sand sheet is exposed between Maullín events D and C (Figs. S2, S3 of Cisternas et al. (2005)). In both stratigraphic level and thickness, the thin sand sheet at Cocotué greatly resembles the sand sheet at Maullín.

The age of the next prominent earthquake and tsunami at Cocotué is AD 1300–1398 (event C), probably several decades after cd. This date overlaps the ages of plants killed by subsidence in Maullín and in Caille (Atwater et al., 2013) and an inferred age in Chucalén. The age of C also overlaps the date of the second oldest large turbidite of Calafquén Lake and the oldest of Riñihue Lake (Moernaut et al., 2014; Tables 1 and S1).

Following event C, a pair of lesser earthquakes and tsunamis left less distinct layers in Cocotué (bc1 and bc2). Notably, turbidites in Calafquén show a similar pattern with evidence of a pair of smaller earthquakes between the events linked to events C and B at Cocotué (Table 1). Radiocarbon dating of the earlier event in Cocotué, bc1, yielded an age (AD 1305–1435) that is indistinguishable from that of event C, while the age of the later bc2 event (AD 1505–1802), is also indistinguishable from that of event B. The similarity in ages together with their stratigraphic proximity (see Fig. 4c) suggests events C, bc1, bc2 and B all occurred close in time. Varve counting in Calafquén Lake supports this inference. The counterpart of bc1 in Calafquén was dated at AD 1460–1470, roughly a century after event C, and bc2 was dated at AD 1544–1548, a few decades before the occurrence of event B.

Event B, another 1960-type earthquake and tsunami, struck Cocotué in AD 1412–1625 (Tables 1 and S1). This age range overlaps with ages of the plant remains that underlie the penultimate tsunami deposit at Maullín and the penultimate large turbidites in Calafquén, Riñihue and Villarrica lakes (Moernaut et al., 2014). Event B at Cocotué likely represents the giant and well-documented Chilean earthquake and tsunami of 1575.

The penultimate event recorded in Cocotué (ab), with a maximum age of AD 1505–1949 and most of its probability density between AD 1700 and 1800, represents a relatively smaller earthquake and tsunami. This event likely corresponds to the south-central Chile earthquake and trans-Pacific tsunami of 1837. While the historical earthquake of 1737 also falls within the age range, there is no known report of a tsunami either in Chile or Japan in 1737. Further, written records suggest the effects of the 1737 earthquake were focused in the northern half of the 1960 region, around Valdivia farther north of Cocotué, while the 1837 effects were more evident in the southern half, closer to Cocotué. In addition, the stratigraphic position of contact ab is closer to the upper contact than to the lower 1575 contact, suggesting a temporal proximity to 1960. Finally, because the tsunami deposit is around 4 cm below the soil that contains the deepest *P. radiata* pollen, event ab likely occurred only several decades before AD 1900.

If contact ab records the 1837 earthquake and tsunami, the 1737 earthquake is the only case, in a 1000-year comparison between Cocotué and the lacustrine record farther north, of an incomplete match. From north to south, lakes Villarica, Calafquén and Riñihue

recorded both 1737 and 1837 earthquakes (Moernaut et al., 2014). However, turbidites suggest that the 1737 shaking was stronger in the northernmost lake, Villarica, than in the lakes to the south. This agrees with the northern location of the 1737 earthquake indicated by written records (Cisternas et al., 2005). Thus, the lack of 1737 evidence in Cocotué is consistent with a more northerly location.

Finally, we infer that event A corresponds to the 1960 earthquake and tsunami. Three lines of evidence support this assumption. First, post-1960 airphotos show both a fresh landslide scarp on the slope directly above fan N and its resulting debris-flow deposit resting on the top of the fan itself (Fig. 3b). Second, the soil beneath the correlative sand sheet contains pollen of the introduced *P. radiata*, making the debris-flow and tsunami deposits younger than AD 1900 (Fig. S3). Third, the 1960 mainshock and associated tsunami remain abundantly recorded by geologic evidence of tsunami at Maullín, Caille and Chucalén, and by evidence of shaking in lakes Calafquén, Riñihue and Villarica.

7. Discussion and synthesis

7.1. Greater sensitivity at Cocotué than at nearby coastal sites

The coastal stratigraphy presented above reveals a sequence of four giant earthquakes and tsunamis that likely matches one-for-one with the events dated within the last 1000 years in nearby coastal sites, at Maullín (Cisternas et al., 2005) and Chucalén (Garrett et al., 2015). Additionally, the Cocotué stratigraphy recorded four relatively smaller events, perhaps 1837-type, that match evidence for four smaller earthquakes in three Andean lakes 270–330 km to the northeast (Moernaut et al., 2014).

Unlike Maullín and Chucalén, the ability of Cocotué to record smaller events probably reflects its exposure to open water together with a physiographic setting that promotes the preservation of thin sand layers. Cocotué is more directly exposed to tsunamis (Fig. 1c). While Cocotué faces the open Pacific, Maullín and Chucalén fringe inland waters. Maullín is 8 km upstream along a tidal river and Chucalén is in a semi-enclosed inland water body.

Although open to the sea, the Cocotué sequence was deposited above the highest tides, as judged from its post-1960 elevation and from diatom assemblages, which indicate that sediments accumulated above the reach of tides throughout the last 1000 years. This elevation prevented tides and perhaps storms from reworking the thin sand sheets and the smaller lenses of diamict. Similarly at Maullín, the 1960 sand sheet is preserved best where pasture soils beneath it barely entered the intertidal zone upon subsiding in 1960. Sand on lower surfaces was widely reworked by waves at high tide that have stripped the underlying soil as well (Cisternas et al., 2005). Cocotué escaped such reworking, despite having subsided about a meter in 1960.

Preservation of the evidence of the smaller events at Cocotué was also likely promoted by later debris-flow deposition. The thin sand sheet marking contact cd was later covered by the debris flow of contact C on both fans S and N (Fig. 4). Contacts bc1 and bc2, as a pair, are similarly buried by the debris flow that caps contact ab in two places on fan S, and the sand sheet on contact ab is protected by the 1960 diamict in fan N. Thus, these thin surviving sheets coincide mainly with the debris-flow fans. It is likely that diamicts, being both thick and hard, shielded the underlying sand sheets from later bioturbation and erosion.

7.2. Sources and relative sizes of the largest earthquakes between AD 1000 and 1960

While the new findings are consistent with the previously assumed megathrust origin for the three giant pre-1960 earthquakes, namely D, C and B (1575), their absolute size remains ambiguous due to the lack of geologic and historical evidence from the southern half of the 1960 region (Fig. 6).

The latitudinal extent of the geologic evidence for each of the three giant predecessors to 1960 in Cocotué, Chucalén, Maullín and Calafquén Lake suggests fault rupture at the boundary between the Nazca and South American plates. No intraplate fault could explain strong shaking for 300 km between Cocotué and Calafquén or coastal land-level changes for 350 km between Maullín and Tirúa, in 1575 (Fig. 6b). The tsunami evidence at Cocotué, Chucalén, Maullín, Caulle, and Tirúa also points to megathrust ruptures that warped the floor of the continental shelf and slope to their west.

Could the size of the debris-flow deposits at Cocotué be indicative of the relative size of the earthquakes? Among these deposits, only those of event D rival the one from 1960 in thickness and continuity along the 500-m outcrop. The size of the 1960 diamict, however, was perhaps enhanced by the land-use change and the season when the event occurred. Spanish colonists initiated widespread clearing of the native rain-forest on Chiloé, promoting soil erosion and slope instability (Torrejón et al., 2004). This process significantly increased and accelerated after Chile's independence in 1810 (Torrejón et al., 2011).

Additionally, the 1960 earthquake occurred during the austral winter, a very rainy season at Chiloé. By contrast, the 1575 earthquake occurred early in the era of land clearing and during the drier austral summer.

Written evidence for far-field tsunamis in Japan, as in 1837 and 1960, could help to define the size of the predecessors to the 1960 earthquake. However, no such evidence has been found in Japan for the 1575 Chilean tsunami (Ninomiya, 1960; Iida et al., 1967; Soloviev and Go, 1984; Watanabe, 1998), despite Chilean written and geologic evidence indicating that the effects of the 1575 earthquake resembled those in 1960. Similarly, there are no accounts in Japan of flooding and damage at times corresponding to the earlier Cocotué events D or C. This lack of Japanese written records is inconclusive, however, because during most of the time interval spanned by events D, C and B (1575), Japan produced few records of natural disasters as the Japanese were immersed in feudal wars (Ueda and Usami, 1990). Still, at least one written record of flooding north of Sendai, at Minami Sanriku, was linked to the 1586 tsunami from Peru. Notably, the 1960 Chilean tsunami was as much as 5 m high in this area (Ninomiya, 1960; Watanabe, 1998).

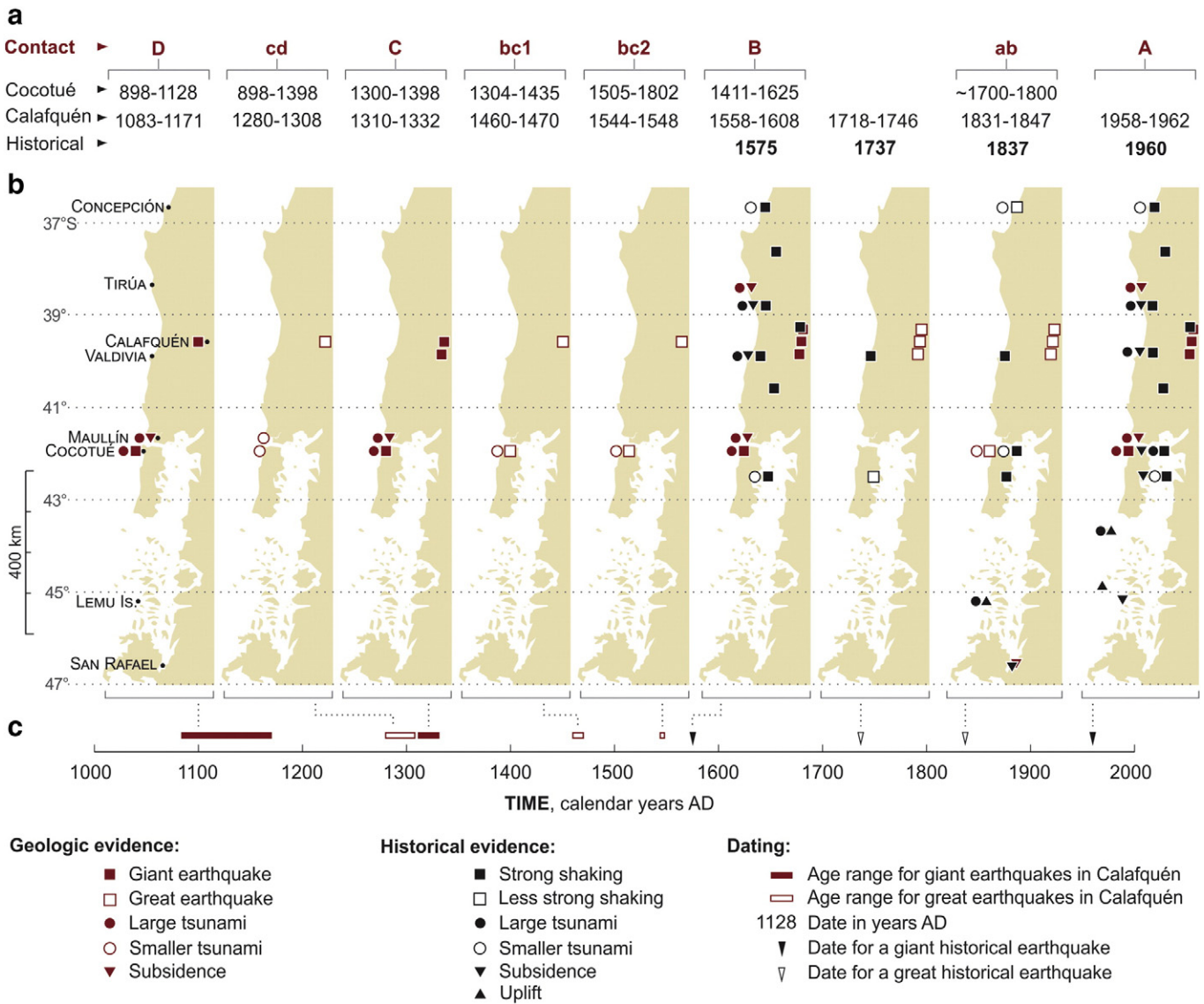


Fig. 6. Graphical summary of the inferred 1000-year earthquake history along the length of the 1960 region. a) Age sequence of the 1960-type and relatively smaller earthquakes recorded at Cocotué compared with ages from Calafquén Lake (Moernaut et al., 2014) and historical dates (Lomnitz, 1970). b) Plot of the stratigraphic and historical evidence for each event. Geologic evidence from Ely et al. (2014), Moernaut et al. (2014), Cisternas et al. (2005), Garrett et al. (2015) and this report. Historical evidence from Lomnitz (1970) and Table S1 of Cisternas et al. (2005). c) Timeline of giant and great earthquakes that struck south-central Chile during the last 1000 years. Age ranges from Calafquén Lake (Moernaut et al., 2014).

7.3. Sources and sizes of the relatively smaller prehistoric earthquakes and tsunamis

Rupture on the megathrust also best explains all three of the relatively smaller, 1837-type, prehistoric events (cd, bc1, and bc2) evidenced at Cocotué and in Calafquén Lake. We consider other offshore sources, such as outer-rise or splay fault ruptures, as unlikely, because the earthquakes were able to produce strong shaking not only on the coast but also in the far inland Andean lakes; a result difficult to explain through secondary offshore faults.

The earliest 1837-type event (cd) is marked by a tsunami deposit in Cocotué and likely in Maullín. However, no evidence for coincident shaking was found in Cocotué. This points to a more distant source, likely in the northern half of the 1960 region where the Calafquén Lake did record correlative shaking. Alternatively, dry conditions not favoring slope instability at Cocotué at the time of the earthquake could also explain such absence.

The pair of events bc1 and bc2, between events C and 1575, is marked by evidence for both shaking and tsunami at Cocotué and for shaking at Calafquén. In this respect each of them resemble the 1837 earthquake (Fig. 6).

7.4. Notably short earthquake recurrence intervals between AD 1300 and 1575

The earthquake recurrence intervals among C, bc1, bc2, and 1575 are remarkably short (Table 1; Fig. 6c). If the date range for event C as indicated by the turbidite record is correct (AD 1310–1332), and event B is in fact 1575, the middle and northern thirds of the 1960 region were struck by at least four megathrust earthquakes and four ensuing tsunamis in just two and a half centuries.

The average recurrence interval for this period (85 yr) is shorter than the historical average in the series 1575, 1737, 1837, 1960 (128 yr) and about three times shorter than the earthquakes geologically recorded at Maullín (285 yr). Furthermore, the interval between event bc2 and 1575 appears to be even shorter than the roughly 85-year average. Correlated with a Calafquén turbidite, bc2 is bracketed by AD 1544–1548. It would imply that the giant 1575 event was preceded by a 1837-type event (bc2) only 30 years before. Although close in time to the foundation of Valdivia in 1552, the first Spanish settlement south of Concepción (Cisternas et al., 2012), bc2 was probably a few years too early to have entered written history through Spanish colonists.

Alternatively, the AD 1300–1575 recurrence story is oversimplified if events bc1 and bc2 ruptured different portions along the area broken in 1960, as likely occurred in 1737 and 1837. While the rupture in 1737 focused in the north, the one in 1837 was in the center and south. If bc1 and bc2 behaved in a similar way, the AD 1300–1575 average recurrence interval for a given portion of the megathrust would be longer than 85 years. However, the pair bc1–bc2 left a geologic imprint far different from that of the 1737–1837 pair in Cocotué. While the 1737 event did not leave any record, the 1837 event is marked by evidence of shaking (debris-flow deposit) and tsunami (sand sheet). In this respect, the geologic record at Cocotué differentiates between these two ruptures. On the contrary, both bc1 and bc2 are clearly and similarly marked by both shaking and tsunamis at Cocotué. It strongly suggests that the bc1 and bc2 ruptures were both similar to that in 1837 and that they occurred if not in the same area, at least nearby.

Consequently, the short bc2–1575 interval provides an important precedent for a recurrence interval comparable to the 56 years that have elapsed since 1960. This inference gives some cause for concern, because by 2011 the accumulated interplate moment deficit showed that locked segments of the 1960 region were already capable of nucleating earthquakes of magnitude 8 (Moreno et al., 2011).

8. Conclusions

The unusual coastal sedimentary record at Cocotué, which combines evidence for seismic shaking and coincident tsunami inundation since AD 1000 in the region of the giant 1960 Chile earthquake, reveals differences in earthquake size and recurrence between successive ruptures.

In the millennium preceding 1960, south-central Chile was struck by three earthquakes that probably resembled the 1960 mainshock (in AD 898–1128, 1300–1398 and 1575) and by five intervening earthquakes that were likely smaller in fault-rupture area. All but one, in 1737, generated obvious tsunamis. This inferred seismic history begins with a giant, 1960-type, earthquake early in the 12th century AD. A relatively smaller earthquake with a tsunami followed before the end of the 13th century. Soon after, early in the 14th century, another giant earthquake was accompanied by a tsunami and may have occurred close in time with a volcanic eruption as well. Two relatively smaller earthquakes and tsunamis ensued between this event and the giant 1575 earthquake and tsunami. The smaller historical events of 1737 and 1837, rupturing different portions of the plate boundary, then failed to expend most of the accumulated plate convergence that contributed to the enormity of the 1960 earthquake.

Since AD 1000, megathrust earthquakes and tsunamis recurred most often between AD 1300 and 1575. The recurrence intervals averaged about 85 years, a little more than the time already elapsed since 1960. This conclusion is of serious concern for two reasons. First, no earthquake has been expected to occur so soon in the area struck only 56 years ago by an earthquake as large as the 1960 event. Second, plate locking suggests that some segments of the region are already capable of nucleating earthquakes as large as magnitude 8.

This millennial earthquake and tsunami history of one of the world's most active subduction zones adds another example of variable rupture mode, in which earthquake size and recurrence interval vary from one earthquake to the next.

Acknowledgments

This work was funded by Chile's Fondo Nacional de Desarrollo Científico y Tecnológico FONDECYT projects 1110848 and 1150321. Additional support for Ely, Wesson and Dura was provided by NSF projects EAR 1145170 and EAR 1144537, and for Garrett by the Quaternary Research Association and Santander. Initial efforts to clean and survey the Cocotué outcrop were made with M. Lagos and S. Shrinivasalu. Other reconnaissance contributors included M. Shishikura, Y. Sawai, C. Youton, S. Fernando, I. Shiappacasse, K. Jankaew, B. Atwater, A. Prendergast, A. Eipert, E. Yulianto, C.P. Rajendran, and I. Tejakusuma. Initial versions of the manuscript were greatly improved by reviews from B. Atwater. Special acknowledgment is given to R. Witter for his constructive reviews of later versions.

Appendix A. Supplementary data

Supplementary data to this article can be found online at <http://dx.doi.org/10.1016/j.margeo.2016.12.007>.

References

- Abe, K., 1979. Size of great earthquakes of 1837–1974 inferred from tsunami data. *J. Geophys. Res.* 84 (B4), 1561–1568.
- Anderson, T., 1974. The chestnut pollen decline as a time horizon in lake sediments in eastern North America. *Can. J. Earth Sci.* 11, 678–685.
- Ando, M., 1975. Source mechanisms and tectonic significance of historical earthquakes along the Nankai Trough, Japan. *Tectonophysics* 27, 119–140.
- Angermann, D., Klotz, J., Reigber, C., 1999. Space-geodetic estimation of the Nazca–South America Euler vector. *Earth Planet. Sci. Lett.* 171, 329–334.
- Atwater, B., Jiménez, N., Vita-Finzi, C., 1992. Net late Holocene emergence despite earthquake-induced submergence, south-central Chile. *Quat. Int.* 15 (16), 77–85.
- Atwater, B., Cisternas, M., Yulianto, E., Prendergast, A., Jankaew, K., Eipert, A., Fernando, S., Tejakusuma, I., Shiappacasse, L., Sawai, Y., 2013. The 1960 tsunami on beach-ridge

- plains near Maullín, Chile: landward descent, renewed breaches, aggraded fans, multiple predecessors. *Andean Geol.* 40, 393–418.
- Azorquiza, O., 1929. Lota, antecedentes históricos con una monografía de la Compañía Minera e Industrial de Chile, Sociedad Imprenta y Litografía Concepción, Concepción.
- Bartsch-Winkler, S., Schmoll, H., 1993. Evidence for late Holocene relative sea-level fall from reconnaissance stratigraphical studies in an area of earthquake subsided intertidal deposits, Isla Chiloé, southern Chile. In: Frostwick, L.E., Steel, R.J. (Eds.), *Tectonic Controls and Signatures in Sedimentary Successions*. International Association of Seismologists, pp. 91–108.
- Bernhardt, A., Melnick, D., Hebbeln, D., Lückge, A., Strecker, M., 2015. Turbidite paleoseismology along the active continental margin of Chile-Feasible or not? *Quat. Sci. Rev.* 120, 71–92.
- Blumberg, S., Lamy, F., Arz, H., Ehtler, H., Wiedicke, M., Haug, G., Oncken, O., 2008. Turbiditic trench deposits at the South-Chilean active margin: a Pleistocene-Holocene record of climate and tectonics. *Earth Planet. Sci. Lett.* 268, 526–539.
- Cifuentes, I., 1989. The 1960 Chilean earthquakes. *J. Geophys. Res.* 94 (B1), 665–680.
- Cisternas, M., Araneda, A., Martínez, P., 2001. Effects of historical land use on sediment yield from a lacustrine watershed in Central Chile. *Earth Surf. Process. Landf.* 26, 63–76.
- Cisternas, M., Atwater, B., Torrejón, F., Sawai, Y., Machuca, G., Lagos, M., Eipert, A., Youlton, C., Salgado, I., Kamataki, T., Shishikura, M., Rajendran, C.P., Malik, J.K., Rizal, Y., Husni, M., 2005. Predecessors of the giant 1960 Chile earthquake. *Nature* 437, 404–407.
- Cisternas, M., Torrejón, F., Gorigoitia, N., 2012. Amending and complicating Chile's seismic catalog with the Santiago earthquake of 7 August 1580. *J. S. Am. Earth Sci.* 33, 102–109.
- Coan, T., 1882. *Life in Hawaii: An Autobiographic Sketch of Mission Life and Labors*. (Available at <http://www.soest.hawaii.edu/gg/hcv/coan/iv.html>).
- Contesse, D., 1987. Apuntes y consideraciones para la historia del Pino radiata en Chile. *Boletín de la Academia Chilena de la Historia* 97, 351–373.
- Darwin, C., 1851. *Geological Observations on South America, Part III—Being the Geology of the Voyage of the Beagle, Under the Command of Captain Fitzroy, R.N., During the Years 1832 to 1836*. Smith, Elder and Co., London.
- Davis, S., Karzulovic, K., 1963. Landslides at Lago Riñihue, Chile. *Bull. Seismol. Soc. Am.* 53 (6), 1403–1414.
- Dawson, S., 2007. Diatom biostratigraphy of tsunami deposits: examples from the 1998 Papua New Guinea tsunami. *Sediment. Geol.* 200, 328–335.
- Donoso, C., Lara, A., 1996. Utilización de los bosques nativos en Chile: pasado, presente y futuro. In: Armesto, J., Villagrán, C., Arroyo, M. (Eds.), *Ecología de los bosques nativos de Chile*. Editorial Universitaria, Santiago, pp. 234–255.
- Dupré, M., 1992. *Palinología*. Geoforma Ediciones, Zaragoza, Spain.
- Dura, T., Hemphill-Haley, E., Sawai, Y., Horton, B., 2016. The application of diatoms to reconstruct the history of subduction zone earthquakes and tsunamis. *Earth Sci. Rev.* 152, 181–197.
- Eaton, J., Richter, D., Ault, W., 1961. The tsunami of May 23, 1960, on the Island of Hawaii. *Bull. Seismol. Soc. Am.* 51, 135–157.
- Egbert, S., Erofeeva, S., 2002. Efficient inverse modeling of barotropic ocean tides. *J. Atmos. Ocean. Technol.* 19, 183–204.
- Egbert, G., Bennett, A., Foreman, M., 1994. Topex/Poseidon tides estimated using a global inverse model. *J. Geophys. Res.* 99 (C12), 24821–24852.
- Ely, L., Cisternas, M., Wesson, R., Dura, T., 2014. Five centuries of tsunamis and land-level changes in the overlapping rupture area of the 1960 and 2010 Chilean earthquakes. *Geology* 42 (11), 995–998.
- Faegri, K., Iversen, J., 1975. *Textbook of Pollen Analysis*. Hafner, New York.
- Garrett, E., Shennan, I., Woodroff, S., Cisternas, M., Hocking, P., Gulliverd, P., 2015. Reconstructing paleoseismic deformation, 2: 1000 years of great earthquakes at Chualén, south central Chile. *Quat. Sci. Rev.* 113, 112–122.
- Goto, K., Sugawara, D., Abe, T., Haraguchi, T., Fujino, S., 2012. Liquefaction as an important source of the A.D. 2011 Tohoku-oki tsunami deposits at Sendai Plain, Japan. *Geology* 40, 887–890.
- Hartley, B., Barber, H., Carter, J., 1996. *An Atlas of British Diatoms*. Biopress, Bristol.
- Hemphill-Haley, E., 1993. Taxonomy of recent and fossil (Holocene) diatoms (Bacillariophyta) from northern Willapa Bay, Washington. *US Geological Survey Open File Report* 93–289, pp. 1–151.
- Hemphill-Haley, E., 1996. Diatoms as an aid in identifying late-Holocene tsunami deposits. *The Holocene* 6 (4), 439–448.
- Heusser, C., 1990. Chilotan piedmont glacier in the southern Andes during the last glacial maximum. *Revista Geológica de Chile* 17, pp. 3–18.
- Heusser, C., Foster, R., 1977. Quaternary glaciations and environments of northern Isla Chiloé, Chile. *Geology* 5, 305–308.
- Hogg, A., Hua, Q., Blackwell, P., Niu, M., Buck, C., Guilderson, T., Heaton, T., Palmer, J., Reimer, P., Reimer, R., Turney, C., Zimmerman, S., 2013. SHCal13 southern hemisphere calibration, 0–50,000 Years cal BP. *Radiocarbon* 55, 1889–1903.
- Hong, I., Dura, T., Ely, L., Horton, B., Nelson, A., Cisternas, M., Nikitina, D., Wesson, R., 2016. A 600-year-long stratigraphic record of tsunamis in south-central Chile. The Holocene <http://dx.doi.org/10.1177/0959683616646191>.
- Iida, K., Cox, D., Pararas-Carayannis, G., 1967. Preliminary Catalog of Tsunamis Occurring in the Pacific Ocean, HIG-67-10. Hawaii Institute of Geophysics, University of Hawaii, Honolulu, Hawaii (275 pp).
- Kanamori, H., McNally, K., 1982. Variable rupture mode of the subduction zone along the Ecuador-Colombia coast. *Bull. Seismol. Soc. Am.* 72, 1241–1253.
- Kempt, L., Anderson, T., Thomas, R., Mudrochova, A., 1974. Sedimentation rates and recent sediment history of lakes Ontario, Erie and Huron. *J. Sediment. Petrol.* 44, 207–218.
- Lomnitz, C., 1970. Major earthquakes and tsunamis in Chile during the period 1535 to 1955. *Geol. Rundsch.* 59, 938–960.
- Lomnitz, C., 2004. Major earthquakes of Chile: a historical survey 1535–1960. *Seismol. Res. Lett.* 75, 368–378.
- Lowe, R., 1974. Environmental requirements and pollution tolerance of freshwater diatoms. US Environmental Protection Agency report EPA-670/4-74-005.
- Melnick, D., Cisternas, M., Moreno, M., Norambuena, R., 2012. Estimating coseismic coastal uplift with an intertidal mussel: calibration for the 2010 Maule Chile earthquake (Mw = 8.8). *Quat. Sci. Rev.* 42, 29–42.
- Moernaut, J., De Batist, M., Charlet, F., Heirman, K., Chapron, E., Pino, M., Brummer, R., Urrutia, R., 2007. Giant earthquakes in South-Central Chile revealed by Holocene mass-wasting events in Lake Puyehue. *Sediment. Geol.* 195, 239–256.
- Moernaut, J., Van Daele, M., Heirman, K., Fontijn, K., Strasser, M., Pino, M., Urrutia, R., de Batist, M., 2014. Lacustrine turbidites as a tool for quantitative earthquake reconstruction: new evidence for a variable rupture mode in south central Chile. *J. Geophys. Res.* 119, 1607–1633.
- Moreno, M., Melnick, D., Rosenau, M., Bolte, J., Klotz, J., Ehtler, H., Baez, J., Bataille, K., Chen, J., Bevis, M., Hase, H., Oncken, O., 2011. Heterogeneous plate locking in the South-Central Chile subduction zone: building up the next great earthquake. *Earth Planet. Sci. Lett.* 305 (3–4), 413–424.
- Nelson, A., Kashima, K., Bradley, L., 2009. Fragmentary evidence of great earthquake subsidence during Holocene Emergence, Valdivia Estuary, South Central Chile. *Bull. Seismol. Soc. Am.* 99, 71–86.
- Nentwig, V., Tsukamoto, S., Frechen, M., Bahlburg, H., 2015. Reconstructing the tsunami record in Tirúa, Central Chile beyond the historical record with quartz-based SAR-OSL. *Quat. Geochronol.* 30 (B), 299–305.
- Ninomiya, S., 1960. Tsunami in Tohoku coast induced by earthquake in Chile; a chronological review. *Tohoku Kenkyu.* 10, pp. 19–23 [in Japanese with English summary].
- Palmer, A., Abbott, W., 1986. Diatoms as indicators of sea level change. In: Van de Plassche, O. (Ed.), *Sea Level Research: A Manual for the Collection and Evaluation of Data*. Geobooks, Norwich, pp. 457–488.
- Plafker, G., Savage, J., 1970. Mechanisms of Chilean earthquakes of May 21 and May 22, 1960. *Geol. Soc. Am. Bull.* 81, 1001–1030.
- Porter, S., 1981. Pleistocene glaciation in the southern Lake District of Chile. *Quat. Res.* 16, 263–292.
- Reed, D., Muir-Wood, R., Best, J., 1988. Earthquakes, rivers and ice: scientific research at the Laguna San Rafael, Southern Chile, 1986. *Geogr. J.* 154 (3), 392–405.
- Rivera, P., Valdebenito, H., 1979. Diatomas recolectadas en las desembocaduras de los ríos Chivilingo, Laraquete y Carampangue, Chile. *Gayana Botánica* 35 pp. 1–97.
- Satake, K., 2014. Advances in earthquake and tsunami sciences and disaster risk reduction since the 2004 Indian Ocean tsunami. *Geosci. Lett.* 1–15.
- Satake, K., Atwater, F., 2007. Long-term perspectives on giant earthquakes and tsunamis at subduction zones. *Annu. Rev. Earth Planet. Sci.* 35, 274–349.
- Sievers, H., 1963. The seismic sea wave of 22 May 1960 along the Chilean coast. *Bull. Seismol. Soc. Am.* 53 (6), 1125–1190.
- Soloviev, S., Go, C., 1984. *Catalogue of Tsunamis on the Western Shore of the Pacific Ocean*. Academy of Science of the USSR, Nauka Publishing House, Moscow (1974). Translated from Russian to English by Canadian Institute for Science and Technical Information, No. 5077, National Research Council, Ottawa, Canada, 1984, 439 pp).
- St-Onge, G., Chapron, E., Mulsow, S., Salas, M., Viel, M., Debret, M., Foucher, A., Mulder, T., Winiarski, T., Desmet, M., Costa, P., Gahleb, B., Jaouen, A., Locat, J., 2012. Comparison of earthquake-triggered turbidites from the Saguenay (Eastern Canada) and Reloncavi (Chilean margin) Fjords: implications for paleoseismicity and sedimentology. *Sediment. Geol.* 243, 89–107.
- Torrejón, F., Cisternas, M., Araneda, A., 2004. Efectos ambientales de la colonización española desde el río Maullín al archipiélago de Chiloé, sur de Chile. *Rev. Chil. Hist. Nat.* 77, 661–677.
- Torrejón, F., Cisternas, M., Alvia, I., Torres, L., 2011. Consecuencias de la tala maderera colonial en los bosques de alerce de Chiloé, sur de Chile (Siglos XVI–XIX). *Magallania* 39, 75–95.
- Udiás, A., Madariaga, R., Buforn, E., Muñoz, D., Ros, M., 2012. The large Chilean historical earthquakes of 1647, 1657, 1730 and 1751 from contemporary documents. *Bull. Seismol. Soc. Am.* 102 (4), 1639–1653.
- Ueda, K., Usami, T., 1990. Changes in the yearly number of historical earthquakes in Japan. *Rekishi Jishin.* 6, pp. 181–187 [in Japanese].
- Van Dam, H., Mertens, A., Sinkeldam, J., 1994. A coded checklist and ecological indicator values of freshwater diatoms from the Netherlands. *Neth. J. Aquat. Ecol.* 28 (1), 117–133.
- Vidal Gormaz, F., 1877. Hundimiento o solevantamiento de los archipiélagos australes de Chile. Memoria premiada por la Universidad de Chile en 1877, Santiago, Imprenta Mejía, p. 1901.
- Watanabe, H., 1998. *Comprehensive List of Destructive Tsunamis to Hit the Japanese Islands*. Univ. Tokyo Press, Tokyo [in Japanese].
- Weischet, W., 1963. Further observations of geologic and geomorphic changes resulting from the catastrophic earthquake of May 1960, in Chile. *Bull. Seismol. Soc. Am.* 53 (6), 1237–1257.